01 Sep 2015

Shear Lag Sutures: Improved Suture Repair through the use of Adhesives

S. W. Linderman

I. Kormpakis

R. H. Gelberman

Victor Birman
Missouri University of Science and Technology, vbirman@mst.edu

et. al. For a complete list of authors, see https://scholarsmine.mst.edu/mec_aereng_facwork/3738

Recommended Citation

S. W. Linderman et al., "Shear Lag Sutures: Improved Suture Repair through the use of Adhesives," *Acta Biomaterialia*, vol. 23, pp. 229-239, Elsevier, Sep 2015.
The definitive version is available at https://doi.org/10.1016/j.actbio.2015.05.002

Published in final edited form as:
Acta Biomater. 2015 September 1; 23: 229–239. doi:10.1016/j.actbio.2015.05.002.

Shear lag sutures: Improved suture repair through the use of adhesives

Stephen W. Linderman[a,b], **Ioannis Kormpakis**[a], **Richard H. Gelberman**[a], **Victor Birman**[c], **Ulrike G. K. Wegst**[d], **Guy M. Genin**[e,*], and **Stavros Thomopoulos**[a,b,e,*]

[a]Department of Orthopaedic Surgery, Washington University, St Louis, MO 63110

[b]Department of Biomedical Engineering, Washington University, St Louis, MO 63130

[c]Engineering Education Center, Missouri University of Science and Technology, St Louis, MO 63131

[d]Thayer School of Engineering, Dartmouth College, Hanover, NH 03755

[e]Department of Mechanical Engineering and Materials Science, Washington University, St Louis, MO 63130

Abstract

Suture materials and surgical knot tying techniques have improved dramatically since their first use over five millennia ago. However, the approach remains limited by the ability of the suture to transfer load to tissue at suture anchor points. Here, we predict that adhesive-coated sutures can improve mechanical load transfer beyond the range of performance of existing suture methods, thereby strengthening repairs and decreasing the risk of failure. The mechanical properties of suitable adhesives were identified using a shear lag model. Examination of the design space for an optimal adhesive demonstrated requirements for strong adhesion and low stiffness to maximize the strength of the adhesive-coated suture repair construct. To experimentally assess the model, we evaluated single strands of sutures coated with highly flexible cyanoacrylates (Loctite 4903 and 4902), cyanoacrylate (Loctite QuickTite Instant Adhesive Gel), rubber cement, rubber/gasket adhesive (1300 Scotch-Weld Neoprene High Performance Rubber & Gasket Adhesive), an albumin-glutaraldehyde adhesive (BioGlue), or poly(dopamine). As a clinically relevant proof-of-concept, cyanoacrylate-coated sutures were then used to perform a clinically relevant flexor digitorum tendon repair in cadaver tissue. The repair performed with adhesive-coated suture had significantly higher strength compared to the standard repair without adhesive. Notably, cyanoacrylate provides strong adhesion with high stiffness and brittle behavior, and is therefore not an ideal adhesive for enhancing suture repair. Nevertheless, the improvement in repair

[*]Corresponding authors gening@seas.wustl.edu (Guy M. Genin), thomopouloss@wustl.edu (Stavros Thomopoulos).

8. Author contributions

SWL derived the shear lag model with help from VB and GMG. SWL designed and performed all experiments with guidance from ST, RHG, VB, and GMG. IK performed the surgeries and provided input into how to apply adhesives to sutures during surgeries. UGKW provided input and data comparing model results to real material properties. SWL wrote the manuscript, and ST, GMG, IK, RHG, VB, and UGKW provided edits.

properties in a clinically relevant setting, even using a non-ideal adhesive, demonstrates the potential for the proposed approach to improve outcomes for treatments requiring suture fixation. Further study is necessary to develop a strongly adherent, compliant adhesive within the optimal design space described by the model.

Keywords

Adhesive; suture; flexor tendon; shear lag; biomechanics

1. Introduction

Sutures are an age-old technology: they have been used for wound closure for over 5 millennia, dating back to sutures used in ancient Egypt, as described in the Edwin Smith Papyrus from 3000 – 1600 BC [1, 2, 3]. While many improvements in suture materials and intricate knot tying techniques have been introduced over the years, the core method of directly sewing tissues together remains a crude mechanical solution. Sutures typically work in pure tension along most of their length. Tension is transferred to the tissue only at anchor points (Figure 1). High stress concentrations at these anchor points can lead to sutures breaking or cutting through the surrounding tissue. This phenomenon limits the maximum force that can be transferred across the repair site. While current suturing techniques are sufficient to maintain the integrity of many surgical repairs, musculoskeletal tissue reconstruction (e.g., tendon and ligament repair) typically demands strong biomechanical resilience to accommodate activities of daily living without risking rupture. For example, repair-site elongation and rupture rates of up to 48% have been described after flexor tendon repair, even with modern suturing and rehabilitation protocols [4, 5, 6, 7]. Rotator cuff repairs, which require reattachment of materials with disparate mechanical properties (tendon and bone), have recently reported failure rates as high as 94% [8, 9, 10]. Improved suturing schemes would allow for the transfer of greater loads across the repair site, reducing rupture and gap formation between the repaired tissues and improving healing outcomes, not only by strengthening repairs but also by enabling more aggressive rehabilitation protocols. By holding the tissues together for longer time intervals, mechanical solutions that prevent gap formation and development could provide more time for the biological healing response to generate a strong, organized tissue instead of disorganized scar [5, 11, 12].

Here, a new approach is proposed to augment standard suturing technology. Conventional sutures have a relatively large surface area passing through the tendon that is currently not utilized for load transfer. We envision a modified suture with an adsorbed or covalently bound adhesive that tightly binds collagen along the suture’s length, thereby reducing stress concentrations and better distributing load (Figure 1). We hypothesized that adhesives along the length of the suture would transfer load more effectively than conventional suture without adhesive. This improvement in load transfer is expected to result in an improvement in overall repair construct mechanical properties. Note that achieving the full strength of an uninjured tendon is unnecessary, as tendons are over-designed and are typically able to accommodate many times more load than is applied physiologically [13, 14, 15]. We aim to

generate functional repairs that are sufficient to accommodate *in vivo* loads and enhanced rehabilitation protocols. We focus here on single stranded sutures or pseudomonofilament sutures, including multiple strands within an outer casing, because these are used surgically for flexor tendon repair [11].

In order to predict the ability of adhesive-coated sutures to improve load transfer, we employed a shear lag model [16, 17, 18, 19] of suture within a cylindrical tissue (e.g., a tendon). Using this model, we identified desirable adhesive mechanical properties to improve load transfer across a repair site. We then biomechanically tested sutures coated with adhesives to validate the model and experimentally assess the capacity to improve load transfer.

2. Materials and methods

2.1. Terminology

Throughout this paper, “suture” refers to the core strand of suture, “adhesive” refers to the adhesive layer, “assembly” and “adhesive-coated suture” refer to the combination of suture with adhesive surrounding it, and “repair” refers to the complete tissue repair, including several strands of adhesive-coated suture and a region of tissue in which these are embedded. Abbreviations and variables are described in Table 1.

2.2. Ex vivo surgical repair model

To experimentally assess the ability of adhesives to improve load transfer, a number of adhesive coatings were added to single pseudo-monofilament polycaprolactam 4-0 suture strands (Supramid, S. Jackson, Inc., Alexandria, VA) and inserted into tendon tissue prior to performing pullout tests. Single strands without knots were chosen to isolate the effects of the adhesive and mimic the mathematical model as closely as possible. The following adhesives were examined: highly flexible cyanoacrylates (Loctite 4903 and 4902, based on ethyl and octyl cyanoacrylate[20, 21]; Henkel Corporation, Düsseldorf, Germany), cyanoacrylate (Loctite QuickTite Instant Adhesive Gel, based on ethyl cyanoacrylate[22], Henkel Corporation, Düsseldorf, Germany), rubber cement (Elmer’s Rubber Cement; Elmer’s Products, Inc., Columbus, OH), rubber/gasket adhesive (1300 Scotch-Weld Neoprene High Performance Rubber & Gasket Adhesive; 3M, St. Paul, MN), BioGlue (CryoLife Inc., Kennesaw, GA), and polydopamine [23, 24] (Sigma Aldrich, St. Louis, MO). Henkel does not release the exact chemical composition of their products. Of these adhesives, only BioGlue is FDA approved for use inside the body. These commercially available adhesives were chosen solely to assess the concept proposed here, not to promote the use of any particular adhesive clinically. Loctite 4903 and 4902 have shear moduli of 538 MPa and 399 MPa, respectively [25]. BioGlue, rubber cement, and rubber/gasket adhesives [26] have shear moduli on the order of 0.5 - 5 MPa [27, 28, 29]. Suture was passed through cadaveric canine hindpaw flexor digitorum profundus tendons using a French eye needle. All tendons tested in this study were from hindpaws of healthy female adult mongrel dogs from 20-30 kg in weight (Covance Research, Princeton, NJ), taken postmortem from an unrelated project. Canine intrasynovial flexor tendons have been used extensively by our group and others since the early 1960s as a reliable model of human

tendon repair; we expect the results from this model to be comparable to those that would be obtained from human flexor tendon reconstructions [5, 30, 31, 32, 33, 34, 35, 36]. Tendons had elliptical cross sections with major and minor radii approximately 3 mm and 1 mm, respectively. The tendon was first dissected away from surrounding tissue and a complete transection was made in Zone II [37] perpendicular to the long axis of the tendon. Suture was passed from the side of the tendon 10 mm from the site of transection toward the laceration interface. The suture was pulled through the tendon so that only a single suture strand remained within the tendon. In the adhesive-coated suture tests, the adhesive was injected onto the suture and the suture was pulled into place, dragging the adhesive into the tendon. Adhesive that accumulated on the side of the tendon was cleared with gauze soaked in phosphate buffered saline (PBS). The assembly within the tendon was wrapped in PBS-soaked gauze in an airtight tube and then allowed to cure overnight at 4 °C before biomechanical testing. This curing procedure was chosen to ensure that the postmortem tissue *ex vivo* would not rot or deteriorate.

To assess the ability of adhesive to improve load transfer in a clinically relevant setting, cadaveric canine hindpaw flexor digitorum profundus tendons with Zone II lacerations [37] were repaired using an 8-strand Winters-Gelberman repair [11] (n = 11; Supramid 4-0 suture; S. Jackson Inc., Alexandria, VA), as diagrammed in Figure 1 and described previously [38]. Control repairs without adhesive were compared to repairs with Loctite 4903-coated suture. Loctite 4903 was chosen based on results of single suture pullout tests described above. All surgeries were performed by IK, an orthopaedic hand surgeon. For adhesive-augmented repairs, sutures were passed through the tendon following usual surgical technique, then for each suture pass, Loctite 4903 was injected onto the suture strands using a syringe immediately prior to pulling the adhesive-coated suture into its final position. The outside of the tendon was cleaned with PBS-soaked gauze to remove any excess adhesive. Repairs were completed with a continuous, nonlocking peripheral stitch using 5-0 nylon suture, as performed clinically [4, 11, 39, 40]. The repaired tendon and distal phalangeal bone were wrapped in PBS-soaked gauze in an airtight tube and then allowed to cure overnight at 4 °C to prevent tissue deterioration before biomechanical testing.

2.3. Biomechanical testing

Samples were brought to 37 °C prior to biomechanical testing. For single suture strand pullout tests, any suture and adhesive outside of the lateral tendon was first dissected away. This ensured that the effect was due to adhesive along the length of the suture instead of adhesive accumulated at the suture entrance point. Samples were then tested in uniaxial tension on a materials testing frame (ElectroPuls E1000; Instron Corp., Norwood, MA, chosen because of a low noise load cell suitable for distinguishing milli-Newton level forces). The tendon was clamped in a stationary grip so 15 mm of tendon length was exposed. Suture was carefully placed in a jig consisting of a low friction spool and a clamp grip, which was pulled upward at 0.3 mm/s to apply tension to the suture. The gauge length between the tendon and suture grips was 8.5 cm for all samples at the start of the test. Pullout (failure) force of single adhesive-coated suture strands within tendon tissue were determined from the force-elongation curves.

Clinical repairs of cadaveric flexor digitorum profundus tendons were tested as described previously [41, 42, 43, 36]. After preconditioning, samples were pulled in uniaxial tension using a material testing machine (5866; Instron Corp., Norwood, MA, chosen because of a high capacity load cell) at 0.3 mm/s until failure. Strain was determined optically to determine when a physiologically relevant 2 mm gap formed between the repaired tendon ends. Immediately prior to testing, tendons were stained with a speckle pattern of freshly prepared Verhoeff stain to provide a surface texture for optical tracking. Elongation measurements from the material testing machine were synced with optical recordings from a high resolution camera at a frame rate of 4 Hz (illunis, Minnetonka, MN), similar to described previously [44]. Optical tracking of points proximal and distal to the laceration interface enabled accurate determination of local tissue strain. From the force-elongation curves, maximum force, force required to create a 2 mm gap in the repair (a clinically relevant measure of repair strength [5]), and stiffness (slope of the linear region) were determined. From the force-strain curves, strain at 20 N force (approximating strains at physiologically relevant load levels [45, 46]) and resilience (area under the curve until yield) were determined.

2.4. Statistics

Statistical analysis for all experiments was performed by non-parametric Wilcoxon rank-sum using MATLAB. Statistical significance was set at $p < 0.05$ unless otherwise noted.

3. Theory

3.1. Shear lag model

A shear lag model was studied to identify adhesives with desirable properties for suture repair (Appendix A). The model predicted load sharing between the sutures and an idealized isotropic, homogeneous repaired tendon.

The load P_s on an assembly that would cause adhesive failure was estimated from the following expression for the shear stress $\tau(x)$ as a function of the position, x, along a suture (Figure 2):

$$\frac{\tau(x)}{\tau_{ave}} = \frac{\beta_s L}{\chi sinh(\beta_s L)} \left[(\chi - 1) cosh(\beta_s (x - L)) - \left(\frac{P_k}{P_s} \chi - 1 \right) cosh(\beta_s x) \right] \quad (1)$$

where $\tau_{ave} = \frac{P_s}{2\pi r_s L}$ is the average shear stress; L is the suture purchase length (i.e., the length of the straight section of the suture within the connected section of the tendon); P_k is the resultant normal force in the suture at the anchor point (the knot at $x = L$); P_s is the normal force in the suture at the interface ($x = 0$); and χ and the characteristic (inverse) length scale β_s relate to the geometry and material properties:

$$\chi = 1 + \frac{\rho_t^{*2}}{E_s^*} \quad (2)$$

$$\beta_s^2 = \frac{1}{r_s^2}\frac{2G_a^*}{t_a^*}\left(\frac{1}{\rho_t^{*2}} + \frac{1}{E_s^*}\right) \quad (3)$$

where $\rho_t^{*2} = r_t^{*2} - (1+t_a^*)^2$, in which $r_t^* \quad and \quad t_a^*$ are, respectively, the tendon radius and adhesive thickness normalized by the suture radius r_s; and $E_s^* \quad and \quad G_a^*$ are, respectively, the suture elastic modulus and adhesive shear modulus normalized by the tendon elastic modulus E_t. The peak shear stress in the adhesive occurs at the interface $x = 0$ (Figure 3). Equating this to the adhesive failure shear stress, τ_{fail}, and solving (1) for the case of $P_k = 0$ yields:

$$\left(\frac{P_{max}}{2\pi r_s^2}\right) = \tau_{fail}\frac{L}{r_s}\frac{sinh\left(\beta_s L\right)}{\beta_s L}\frac{\chi}{\left(\chi - 1\right)cosh\left(-\beta_s L\right) + 1} \quad (4)$$

Note that τ_{fail} could be limited by failure at the interfaces with adherends (i.e., suture or surrounding tissue) or failure within the adherends themselves. This solution is nearly bilinear, with two asymptotes (Figure 4, Figure 5):

$$\lim_{L\to\infty}\left(\frac{P_{max}}{2\pi r_s^2}\right) = \tau_{fail}\left[\frac{E_s^* t_a^*}{2G_a^*}\left(1 + \frac{E_s^*}{\rho_t^{*2}}\right)\right]^{\frac{1}{2}} \quad (5)$$

$$\lim_{G_a\to\infty}\left(\frac{P_{max}}{2\pi r_s^2}\right) = \tau_{fail}\frac{L}{r_s} \quad (6)$$

For a given suture, the first limit ($L \to \infty$) shows that the force a suture can carry increases monotonically with decreasing adhesive shear modulus G_a^*. Below a critical adhesive shear modulus, however, the second limit ($G_a \to 0$) shows that a cut-off exists that depends upon the suture length. Therefore, the optimum strength involves as compliant of an adhesive provided that the suture length is sufficient:

$$L \geq L_{intersect} \equiv r_s\left[\frac{E_s^* t_a^*}{2G_a^*}\left(1 + \frac{E_s^*}{\rho_t^{*2}}\right)\right]^{\frac{1}{2}} \quad (7)$$

As a test case for a clinically relevant suture repair scenario, the model was analyzed using realistic tendon and suture material properties and a variety of realistic suture lengths and adhesive properties for a typical flexor digitorum profundus clinical repair: L = 13 mm, r_t = 2 mm, E_t = 200 MPa, t_a = 100 μm, r_s = 100 μm, and E_s = 2 GPa [38, 47, 48, 49, 50, 51, 52].

4. Results

4.1. Shear lag model analysis

Shear lag modeling predicted that adhesive coatings on sutures would improve load transfer compared to conventional sutures for a certain range of properties (white band, Figure 4). Mechanically desirable adhesives would be compliant in shear while maintaining high binding and shear strengths. Compliant adhesives allow greater deformation, thereby

distributing loads over a larger length than stiff adhesives (Figure 3a). This distribution reduces stress concentrations at the suture anchor points, leading to an adhesive-coated suture assembly that carries greater load before failure. In addition to adhesive properties, the maximum shear stress in the adhesive is minimized by balancing the adherends [53] (i.e., tissue and suture) so that $E_s^* = \rho_t^{*2}$. These adherends are not balanced with current Supramid surgical suture and tendon. When adherends (tendon and suture) are balanced by assuming 38-fold stiffer suture, the peak stress is 8.5-fold lower than in conventional suture repair (Figure 3b).

Shear lag modeling also predicted that maximum load transfer would increase with increasing adhesive-coated suture length. However, varying the ratio of suture length to $L_{intersect}$ demonstrates that adhesive-coated sutures approach the limit for maximum load transferred when the suture length, L, is 2-3 times $L_{intersect}$ (Figure 5a). The length of suture used is limited surgically by the particular tissue being repaired. Suture length of 13 mm was used in the model to make results relevant to flexor digitorum profundus tendon repair (Figure 5b) [39]. A contour map of maximum load transfer given various adhesive properties was generated using this length (Figure 4). Properties of several real materials were then overlaid on this contour map to identify promising candidate materials. Only a small fraction of the material classes shown are relevant materials; the remainder are included for comparison as is standard with an Ashby plot, and to highlight the importance of appropriate adhesive material selection. Assuming a compliant adhesive (G_a = 100 kPa) with a strong shear strength (τ = 10 MPa) and the current clinical suture length of 13 mm, maximum load transfer per strand would approach 70 N of force. For the typical 4- and 8-strand methods used in flexor tendon repair, this would result in theoretical improvements of up to 280 N and 560 N, ~4-fold and ~8-fold improvements over current methods, respectively.

4.2. Ex vivo experimental results

Biomechanical tests of single strands of adhesive-coated suture within tendon tissue supported the model prediction that adhesive coatings can increase force required to pull out a suture. Loctite 4903, a “flexible” cyanoacrylate, improved the maximum load to pull out a single suture strand in tendon from 0.076 N (± 0.104 N standard deviation) without adhesive to 3.24 N (± 2.11 N; $p = 3.11 * 10^{-4}$) with an adhesive-coated suture strand (Figure 6). The more compliant adhesives tested did not meaningfully increase the maximum load necessary to pull out the suture, likely because of poor binding to suture and tissue.

The strongest single strands of adhesive-coated suture in tendon were further evaluated in a clinically relevant 8-stranded cadaveric canine flexor tendon repair. Since the results for Quicktite, Loctite 4902, and Loctite 4903 were comparable, the choice among them was arbitrary from the mechanics perspective. In the clinically relevant *ex vivo* repairs, Loctite 4903-coated sutures increased maximum load transfer by 17.0% (Control = 72.7 ± 11.3 N; Loctite 4903 = 85.0 ± 8.6 N; $p = 0.009$) and load to create a clinically relevant 2 mm gap by 17.5% (Control = 59.2 ± 8.8 N; Loctite 4903 = 69.5 ± 11.2 N; $p = 0.032$) compared to standard 8-stranded suture repairs without adhesive coatings (Figure 7; $n = 11$ per group). Resilience, stiffness, and strain at 20 N applied force did not change significantly (Table 2).

5. Discussion

Although adhesives, especially cyanoacrylates [58], have been used for decades in surgical repairs to replace or augment suture for closing the skin and other tissues [59, 60], their application has been almost entirely limited to the interface between the aligned tissues. The application of adhesive to the lateral faces of sutures has never been reported for a tissue that works in tension. To our knowledge, only one previous study used adhesive-soaked sutures, reporting an increase in re-bonding strength of repaired meniscal tissue under compression compared to either suture alone or adhesive alone [61]. We hypothesized that the load distribution along sutures and the load tolerance of the repaired tissues could be optimized using a mechanical model that predicts load transfer as a function of adhesive mechanical properties. Modeling and *ex vivo* experimental results demonstrated that adhesive-coated sutures have the potential to improve the strength of tensile tissue repairs, especially with the development of adhesives with optimal mechanical properties.

The modeling indicated that adhesives that are compliant in shear facilitate load transfer from the suture to the tendon by lowering stress concentrations (Figure 3). This strategy is somewhat analogous to the tendon enthesis, where a compliant interfacial zone between tendon and bone [62, 63, 64] has been shown to optimize stress transfer and is hypothesized to toughen the interface [65]. Similarly, a collagen-binding adhesive that directly attaches to the suture via a small compliant layer in between the suture and the collagen would be expected to better distribute load to minimize stress concentrations, enabling more effective load transfer across the repair. Finally, we note that compliant interfaces between fibers and matrix are associated with additional modes of toughening through crack deflection [66]; this can lead to toughening of the repair as a whole through decreased sensitivity to flaws that might otherwise lead to failure [67, 68].

Adhesives with a broad range of physical properties are expected to improve load repair strength. When the derived isoclines are plotted over the properties of real materials, as in a standard Ashby plot [55, 54, 56], the model highlights a range of potential materials with appropriate mechanical properties (Figure 4). Many of these are not biocompatible, but elastomers such as polychloroprene, polyurethane rubber, and natural rubber do have appropriate shear moduli and shear strength to be used as base materials for adhesive development. Some biological materials, e.g., those based on elastin, could also be valuable for creating bio-adhesives. Note that the shear strength used in this model may be limited by either bulk failure within the adhesive material or interfacial failure between the adhesive and adherends (i.e., suture and tendon). Therefore, both the bulk adhesive mechanical properties and the strength of adhesion are crucial factors for successful application of this approach.

The proof-of-concept experiments performed here demonstrate substantial improvements in load transfer across single strand pullout and clinically relevant tendon repairs, even though Loctite 4903 used in these tests is a stiff cyanoacrylate that is far from ideal according to the shear lag model. The 3.24 N ± 2.11 N failure load found experimentally for a single strand of cyanoacrylate-coated suture within tendon tissue (Figure 6) very closely matches the predicted maximum load for cyanoacrylates from the shear lag model (Figure 4). The 17%

improvement in load tolerance for a complete 8-stranded repair (Figure 7), amounting to improvement of 10–15 N, could substantially decrease rupture rate in flexor tendon repairs. The expected load transfer for clinically relevant repairs comes partially from the shear lag load transfer through adhesive and partially from the basal strength of a suture repair with knots. This 17% improvement in load transfer across a clinically relevant repair represents 47% of the additive improvement expected for an 8-strand repair based on the single strand experiments. We hypothesize that this discrepancy is due to imbalanced load sharing among strands in the surgical repair. Perfectly balanced repairs are not possible even for the highly trained orthopaedic hand surgeons who performed the procedures in this study because they require that (*i*) all strands have the exact same tension applied to them when surgical knots are tied, (*ii*) the strands be perfectly aligned with the longitudinal axis of the tendon, and (*iii*) the tendon be loaded perfectly longitudinally. Therefore, some strands will carry more load than others in clinically relevant repairs, reducing the maximum load transfer.

The compliant adhesives tested here did not substantially improve load transfer as anticipated by overlaying their bulk material properties on the shear lag model (Figure 6). This discrepancy highlights the importance of compatibility between the different materials (i.e., suture, adhesive, and tendon) and the resulting interfacial shear strengths. Overall shear strength could be limited by any of three factors: (*i*) the interfacial shear strength between suture and adhesive, (*ii*) the interfacial shear strength between adhesive and surrounding tissue, and (*iii*) the bulk shear strength of the adhesive material. This study experimentally evaluated the model using several commercially available adhesives without prior knowledge of their binding strength to Supramid (polycaprolactam) sutures or tendon tissue. Notably, these commercially available adhesives were not optimized to adhere to suture and tissue, whereas strength parameters used in the model represented an optimal scenario where the interfacial shear strengths were at least as strong as bulk shear strength of the adhesives. Poor binding strength of these commercially available adhesives to suture or tissue might have limited the failure shear stress and efficacy for load transfer. While we tested Supramid sutures because of their surgical use in flexor tendon repair, different suture materials may have improved compatibility with particular adhesives. In addition, multifilament sutures have increased surface area for adhesive integration and binding, serving as a potential mechanism to increase interfacial failure shear stress.

Since adhesives were simply injected onto the suture surface before the suture was pulled into tissue, the compliant adhesives may have sheared off of the suture when pulled into place, before adequately curing could take place. One limitation of this experimental validation is the lack of suitable visualization of adhesive within the tissue along the length of the suture. We hope to overcome this limitation in future work. The modeling performed here is applicable even for thin adhesive layers compared to the tissue and suture width. Furthermore, the methods described above ensure that the effects seen experimentally were due to adhesive along the length of the suture instead of adhesive at the entry point into tissue (Figure 6).

Despite these limitations, the single-strand pullout results for cyanoacrylates were accurately predicted by the mathematical model. This is possibly because Henkel publishes lap shear strength for cyanoacrylates instead of block shear strength, so the shear data includes

interfacial adhesive strength. Additionally, cyanoacrylates are highly reactive compounds that may generate sufficient interfacial adhesive strength via covalent bonding with suture and with tendon that they were instead limited by failure within the adhesive bulk.

The promising mechanical improvement seen in these proof-of-concept studies with sub-optimal adhesives is still an order of magnitude below the predicted improvement that could be achieved with an optimal adhesive. While current repairs are not strong enough to sustain physiologic loading in all patients, even modest mechanical improvements are expected to make a substantial difference clinically. Therefore, we anticipate this technology will be useful clinically even if we only see half of the maximum expected improvement based on single-strand testing for a specifically engineered compliant adhesive material. Note that we do not suggest the specific adhesives tested in this proof-of-concept study be used clinically. Rather, these results provide a foundation for the further development of adhesives with the desirable mechanical properties predicted here, material compatibility with sutures and tissue, delivery methods that mitigate adhesives shearing off of suture, and appropriate biocompatibility for use in patients.

This shear lag model describes the importance of adhesive mechanical properties for creating a successful adhesive-coated suture; however, most currently used adhesives are not designed for this purpose. Specifically engineering an adhesive material to bind suture and surrounding tissue tightly, while maintaining compliance to shear stress, could lead to substantially improved adhesive-coated sutures. In addition to having appropriate mechanical properties once in place, an ideal adhesive-coated suture should be inert for storage and surgical handling before it is placed into the body. We envision several potential approaches to generate adhesive coatings that only activate when in place within tissue.

The shear lag model used in the current study employed several simplifying assumptions. First, shear lag models treat the displacement field as one-dimensional. Only displacements along the long axis of the tendon/suture were considered. This approximation has, however, proven effective for a broad range of fibrous composites [17, 69, 70]. Second, the adhesive layer was considered to be very thin. For a thicker layer, deformation of the adhesive must be considered explicitly, accounting for both axial displacements varying through the thickness as well as radial displacements, especially for highly compliant adhesives. Third, the stress field in the suture was assumed to be independent of radial position, an approximation valid only for relatively stiff sutures. Because non-absorbable sutures used in tendon repair can be assumed rigid in tension in the range of the failure forces of the repair, this approximation should be acceptable, especially for estimates of load transfer. Despite limitations listed above, this simplified model of suture-tendon interaction allows for adequate determination of the design space for an adhesive-coated suture for tissue repair. When used in combination with an Ashby plot showing real material properties [55], this model can identify promising base materials for adhesive-coated suture development.

6. Conclusion

Strengthening surgical repairs should lead to improved healing outcomes for mechanically sensitive tissues, such as tendon. Our models and proof-of-concept experiments suggest that

coating sutures with adhesives that are appropriately designed hold promise for achieving repairs that have higher levels of resistance to gap formation and catastrophic failure. While Loctite 4903 shows promising results that would be valuable clinically, it is far from an ideal adhesive according to the model due to its high shear modulus. We intend to develop biocompatible adhesives with optimized mechanical and chemical properties to further increase load transfer and improve clinical repairs for tendon, ligament, and other tissue injuries.

7. Acknowledgements

This study was supported by the National Institutes of Health (NIH): U01 EB016422 (to ST and GMG), R01 AR062947 (to ST and RHG), T32 AR060719 (to SWL) and T32 GM007200 (to Medical Scientist Training Program, Washington University in St. Louis). Loctite 4902 and 4903 were gifts from Henkel Corporation (Düsseldorf, Germany).

Appendix A: Shear lag analysis of an adhesive suture

The shear lag model applied was analogous to the Volkersen [16] and Cox [17] double lap joint solutions, and to the Nairn [18] axisymmetric solution (cf. Appendix B). We present a derivation here to highlight our approximations and how adhesive properties arise in the final expression.

The model was based upon the free body diagram in Figure A.8) and the following assumptions: (a) the suture, adhesive, and tendon are linear elastic materials; (b) viscous effects are negligible; and (c) radial displacements, strains, and stresses are small. The latter is appropriate for a thin adhesive layer. These validity of these assumptions has been established in composites with short [69, 17] and long fibers (e.g., Gibson [70]), and by comparison to solutions in which these assumptions were not made [71, 72]. We note as well that, although adhesives often exhibit nonlinearity and viscoelasticity, the linear analysis is adequate and useful for the target design range in which the adhesive is not close to failure.

The differential equation governing the normal stress in the suture at position x is [17, 18]:

$$\frac{d^2\bar{\sigma}_s(x)}{dx^2} - \beta_s^2\bar{\sigma}_s(x) + \frac{\beta_s^2}{\chi} = 0 \quad \text{(A. 1)}$$

where $\bar{\sigma}(x)$ is normal stress in the suture normalized by the stress $P_s/\pi r_s^2$ at $x = 0$, and β_s and χ are defined in the main text. Solving and applying the boundary condition $\bar{\sigma}_s(0) = 1$ at the interface between repaired tendon ends and $\bar{\sigma}_s(L) = P_k/P_s$ at the anchor or knot yields:

$$\begin{aligned}\bar{\sigma}_s(x) \quad &= \frac{1}{\chi} + \left(1 - \frac{1}{\chi}\right) cosh(\beta_s x) \\ &+ \frac{sinh(\beta_s x)}{sinh(\beta_s L)} \left(\frac{P_k}{P_s} - \frac{1}{\chi} + \left(\frac{1}{\chi} - 1\right) cosh(\beta_s L)\right)\end{aligned} \quad \text{(A.2)}$$

Inserting this into the equilibrium equation yields an expression for the shear stress $\tau(x)$ (Equation 1).

Note that, as with lap joints (e.g. [53]), parametric analysis of Equation 1 confirmed that peak stress is minimized if the inner and outer adherends (tendon and suture) are "balanced" so that $E_s^*=\rho_t^{*2}$ (Figure 3b). This is not the case for current Supramid surgical suture and tendon. Balancing requires a 38-fold stiffer suture, and would reduce the peak stress by a factor of 8.5 (assuming geometry and material properties used in the main text).

Appendix B: Derivation from Nairn's (1997) general, optimized shear lag solution

Nairn [18] presented a general shear lag solution for n concentric, transversely isotropic cylinders that sustain an average axial stress of σ_0. We verify in this appendix that, for the case of $n = 3$ an expression analogous to that of Appendix A can be derived from this solution. Nairn's governing equation for the interfacial shear stress $\tau_{rz}(r)$ at suture/adhesive interface is:

$$\begin{aligned}&2\left[-\tau_{rz}(r_s)\left(\frac{1}{E_s^*}+\frac{1}{E_a^*(t_a^{*2}+2t_a^*)}\right)+\frac{(1+t_a^*)\tau_{rz}(r_s+t_a)}{E_a^*(t_a^{*2}+2t_a^*)}\right]\\&=-\tau_{rz}^{"}(r_s)\left[\frac{1}{4G_2^*}+\frac{(1+t_a^*)^2}{2G_a^*(t_a^{*2}+2t_a^*)}\left(\frac{(1+t_a^*)^2}{t_a^{*2}+2t_a^*}ln(1+t_a^*)-1+\frac{t_a^{*2}+2t_a^*}{2(1+t_a^*)^2}\right)\right]\\&+\frac{(1+t_a^*)^3\tau_{rz}^{"}(r_s+t_a)}{2G_a^*(t_a^{*2}+2t_a^*)}\left(\frac{1}{t_a^{*2}+2t_a^*}ln(1+t_a^*)-1+\frac{t_a^{*2}+2t_a^*}{2(1+t_a^*)^2}\right)\end{aligned}\quad\text{(B.1)}$$

where G_s^* is the shear modulus of the suture normalized by the elastic modulus of the tendon and all other variables are as defined in Appendix A. For the adhesive/tendon interface,

$$\begin{aligned}&2\left[\frac{\tau_{rz}(r_s)}{E_a^*(t_a^{*2}+2t_a)}-(1+t_a^*)\tau_{rz}(r_s+t_a)\left(\frac{1}{E_a^*(t_a^{*2}+2t_a^*)}+\frac{1}{\rho_t^{*2}}\right)\right]\\&=\frac{\tau_{rz}^{"}(r_s)}{2G_a^*(t_a^{*2}+2t_a^*)}\left(\frac{(1+t_a^*)^2}{t_a^{*2}+2t_a^*}ln(1+t_a^*)-1+\frac{t_a^{*2}+2t_a^*}{2}\right)\\&-(1+t_a^*)\tau_{rz}^{"}(r_s+t_a)\left[\frac{1}{2G_a^*(t_a^{*2}+2t_a^*)}\left(\frac{1}{t_a^{*2}+2t_a^*}ln(1+t_a^*)-1+\frac{t_a^{*2}+2t_a^*}{2}\right)+\frac{r_t^{*2}}{2G_t^*\rho_t^{*2}}\left(\frac{r_t^{*2}}{\rho_t^{*2}}ln\frac{r_t^{*2}}{(1+t_a^*)^2}-1+\frac{\rho_t^{*2}}{2r_t^{*2}}\right)\right]\end{aligned}\quad\text{(B.2)}$$

where G_t^* is the shear modulus of the tendon normalized by the elastic modulus of the tendon.

We model the case of a thin adhesive layer ($t_a^*\ll 1$) that is compliant compared to the suture and tendon ($G_a^*\ll G_s^*\quad and\quad G_a^*\ll G_t^*$). We also assume that the shear stress to be uniform throughout the adhesive layer, as is reasonable for a thin layer. Thus,

$\tau_{rz}(r_s)\approx\tau_{rz}(r_s+t_a)\quad and\quad\tau_{rz}^{"}(r_s)\approx\tau_{rz}^{"}(r_s+t_a)$.

Making the two assumptions noted above and rewriting the above equations in the form

$$\tau_{rz}^{"}-\beta_N^2\tau_{rz}=0$$

yields:

$$\beta_N^2\approx\frac{1}{r_s^2}\frac{2G_a^*}{t_a^*}\left(\frac{1+t_a^*}{\rho_t^{*2}}+\frac{1}{E_s^*}\right)\quad\text{(B.3)}$$

which is equal to the expression in Equation (2) for $t_a^*\ll 1$.

References

[1]. Breasted, JH. The Edwin Smith Surgical papyrus (facsimile and hieroglyphic transliteration with translation and commentary, in two volumes). The University of Chicago Press; Chicago, Illinois: 1930.

[2]. Allen, JP. The Art of Medicine in Ancient Egypt. The Metropolitan Museum of Art; New York, NY: 2005.

[3]. Unknown, Possibly Imhotep (Egyptian Physician), ; 3000 - 1600 B.C.;Edwin Smith Papyrus. URL: http://archive.nlm.nih.gov/proj/ttp/flash/smith/smith.html. URL Accessed: 12/08/2014

[4]. Kim HM, Nelson G, Thomopoulos S, Silva MJ, Das R, Gelberman RH. Technical and biological modifications for enhanced flexor tendon repair. J Hand Surg Am. 2010; 35(6):1031–7. [PubMed: 20513584]

[5]. Gelberman RH, Boyer MI, Brodt MD, Winters SC, Silva MJ. The Effect of Gap Formation at the Repair Site on the Strength and Excursion of Intrasynovial Flexor Tendons. J Bone Joint Surg Am. 1999; 81-A(7):975–982. [PubMed: 10428129]

[6]. Fufa DT, Osei DA, Calfee RP, Silva MJ, Thomopoulos S, Gelberman RH. The effect of core and epitendinous suture modifications on repair of intrasynovial flexor tendons in an in vivo canine model. J Hand Surg Am. 2012; 37(12):2526–31. [PubMed: 23174065]

[7]. Xu C, Zhao J, Li D. Meta-analysis comparing single-row and double-row repair techniques in the arthroscopic treatment of rotator cuff tears. J Shoulder Elbow Surg. 2013; 23(2):1–7. [PubMed: 24200530]

[8]. Galatz LM, Ball CM, Teefey SA, Middleton WD, Yamaguchi K. The outcome and repair integrity of completely arthroscopically repaired large and massive rotator cuff tears. J Bone Joint Surg Am. 2004; 86-A(2):219–24. [PubMed: 14960664]

[9]. Harryman DT II, Mack LA, Wang KY, Jackins SE, Richardson ML, Matsen FA III. Repairs of the rotator cuff. Correlation of functional results with integrity of the cuff. J Bone Joint Surg Am. 1991; 73(7):982–989. [PubMed: 1874784]

[10]. Yamaguchi K, Levine WN, Marra G, Galatz LM, Klepps S, Flatow EL. Transitioning to arthroscopic rotator cuff repair: the pros and cons. Instr Course Lect. 2003; 52(1):81–92. [PubMed: 12690842]

[11]. Winters SC, Gelberman RH, Woo SLY, Chan SS, Grewal R, Seiler JG III. The Effects of Multiple-Strand Suture Methods on the Strength and Excursion of Repaired Intrasynovial Flexor Tendons: A Biomechanical Study in Dogs. J Hand Surg Am. 1998; 23(1):97–104. [PubMed: 9523962]

[12]. Killian ML, Cavinatto L, Shah SA, Sato EJ, Ward SR, Havlioglu N, et al. The effects of chronic unloading and gap formation on tendon-to-bone healing in a rat model of massive rotator cuff tears. J Orthop Res. 2014; 32(3):439–47. [PubMed: 24243733]

[13]. Butler DL, Goldstein S.a. Guilak F. Functional tissue engineering: the role of biomechanics. J Biomech Eng. 2000; 122(6):570–5. [PubMed: 11192376]

[14]. Korvick DL, Cummings JF, Grood ES, Holden JP, Feder SM, Butler DL. The use of an implantable force transducer to measure patellar tendon forces in goats. J Biomech. 1996; 29(4): 557–561. [PubMed: 8964786]

[15]. Juncosa N, West JR, Galloway MT, Boivin GP, Butler DL. In vivo forces used to develop design parameters for tissue engineered implants for rabbit patellar tendon repair. J Biomech. 2003; 36:483–488. [PubMed: 12600338]

[16]. Volkersen V. Die Nietkraftverteilung in zugbeanspruchten Nievtverbindungen mit konstanten Laschenquerschnitten. Luftfahrforschung. 1938; 15:41–47.

[17]. Cox H. The Elasticity and Strength of Paper and Other Fibrous Materials. Br J Appl Phys. 1952; 3(3):72.

[18]. Nairn JA. On the use of shear-lag methods for analysis of stress transfer in unidirectional composites. Mech Mater. 1997; 26(2):63–80.

[19]. Nairn JA, Mendels DA. On the use of planar shear-lag methods for stress-transfer analysis of multilayered composites. Mech Mater. 2001; 33:335–362.

[20]. Henkel Corporation. Technical Data Sheet: Loctite 4902. 2014. URL: https://tds.us.henkel.com/NA/UT/HNAUTTDS.nsf/web/41BCEE769DD0931C85257CF5004876E3/$File/4902-EN.pdf. URL Accessed: 03/25/2015

[21]. Henkel Corporation. Technical Data Sheet: Loctite 4903. 2014. URL: https://tds.us.henkel.com/NA/UT/HNAUTTDS.nsf/web/0192ED8CF7AABF1685257CF50048CB6A/$File/4903-EN.pdf. URL Accessed: 03/25/2015

[22]. Henkel Corporation. Technical Data Sheet: Loctite Quicktite Instant Adhesive Gel. 2005. URL: https://tds.us.henkel.com/NA/UT/HNAUTTDS.nsf/web/A7685691D5C6B064882571870000DC0D/$File/QuicktiteGel-EN.pdf. URL Accessed: 03/25/2015

[23]. Lee H, Dellatore SM, Miller WM, Messersmith PB. Mussel-inspired surface chemistry for multifunctional coatings. Science. 2007; 318(5849):426–30. [PubMed: 17947576]

[24]. Lee H, Lee BP, Messersmith PB. A reversible wet/dry adhesive inspired by mussels and geckos. Nature. 2007; 448(7151):338–41. [PubMed: 17637666]

[25]. Henkel Corporation. Loctite Highly Flexible Instant Adhesives. 2014. URL: http://www.henkelna.com/us/structure_images/11839_LT6864_CHART507316_338984_web_563W.jpg. URL Accessed: 10/06/2014

[26]. 3M Industrial Adhesives and Tapes Division. 3M Scotch-Weld Neoprene High Performance Rubber & Gasket Adhesives - 1300 and 1300L Technical Data. 2012. URL: http://multimedia.3m.com/mws/mediawebserver?mwsId=66666UgxGCuNyXTtnxfVNXz6EVtQEcuZgVs6EVs6E666666--&fn=1300and1300LDataPage_R2.pdf. URL Accessed: 10/14/2014

[27]. Babitt, RO. Vanderbilt Rubber Handbook. 13. R T Vanderbilt; 1990.

[28]. Harper, CA. Handbook of Plastics, Elastomers, and Composites. 3. McGraw Hill; 1996.

[29]. Azadani AN, Matthews PB, Ge L, Shen Y, Jhun CS, Guy TS, et al. Mechanical properties of surgical glues used in aortic root replacement. Ann Thorac Surg. 2009; 87(4):1154–60. [PubMed: 19324142]

[30]. Potenza AD. Detailed evaluation of healing processes in canine flexor digital tendons. Mil med. 1962; 127:34–47. [PubMed: 14488262]

[31]. Potenza AD. Tendon healing within the flexor digital sheath in the dog. The Journal of Bone & Joint Surgery. 1962; 44-A(1):49–64. [PubMed: 14038468]

[32]. Gelberman RH, Menon J, Gonsalves M, Akeson WH. The effects of mobilization on the vascularization of healing flexor tendons in dogs. Clin Orthop Relat Res. 1980; 153:283–289. [PubMed: 7449228]

[33]. Gelberman RH, Woo SL, Lothringer K, Akeson WH, Amiel D. Effects of early intermittent passive mobilization on healing canine flexor tendons. J Hand Surg Am. 1982; 7(2):170–175. [PubMed: 7069172]

[34]. Gelberman RH, Manske PR, Vande Berg JS, Lesker P.a. Akeson WH. Flexor tendon repair in vitro: a comparative histologic study of the rabbit, chicken, dog, and monkey. J Orthop Res. 1984; 2(9):39–48. [PubMed: 6491797]

[35]. Woo SLY, Gelberman RH, Cobb NG, Amiel D, Lothringer K, Akeson WH. The importance of controlled passive mobilization on flexor tendon healing. Acta Orthop Scand. 1981; 52(6):615–622. [PubMed: 7331798]

[36]. Gelberman RH, Thomopoulos S, Sakiyama-elbert SE, Das R, Silva MJ. The Early Effects of Sustained Platelet-Derived Functional and Structural Properties of Repaired Intrasynovial Flexor Tendons : An In Vivo Biomechanic Study at 3 Weeks in Canines. J Hand Surg Am. 2007; 32A(3):373–379. [PubMed: 17336846]

[37]. Kleinert HE, Verdan C. Report of the Committee on Tendon Injuries. J Hand Surg Am. 1983; 8(5):794–798. [PubMed: 6630960]

[38]. Osei DA, Stepan JG, Calfee RP, Thomopoulos S, Boyer MI, Potter R, et al. The Effect of Suture Caliber and Number of Core Suture Strands on Zone II Flexor Tendon Repair: A Study in Human Cadavers. J Hand Surg Am. 2014; 39(2):262–268. [PubMed: 24342261]

[39]. Nelson GN, Potter R, Ntouvali E, Silva MJ, Boyer MI, Gelberman RH, et al. Intrasynovial flexor tendon repair: a biomechanical study of variations in suture application in human cadavera. J Orthop Res. 2012; 30(10):1652–9. [PubMed: 22457145]

[40]. Diao E, Hariharan S, Soejima O, Lotz JC, Francisco S. Effect of Peripheral Suture Depth on Strength of Tendon Repairs. J Hand Surg Am. 1996; 21(2):234–239. [PubMed: 8683052]

[41]. Thomopoulos S, Kim HM, Silva MJ, Ntouvali E, Manning CN, Potter R, et al. Effect of bone morphogenetic protein 2 on tendon-to-bone healing in a canine flexor tendon model. J Orthop Res. 2012; 30(11):1702–9. [PubMed: 22618762]

[42]. Silva MJ, Thomopoulos S, Kusano N, Zaegel MA, Harwood FL, Matsuzaki H, et al. Early healing of flexor tendon insertion site injuries: Tunnel repair is mechanically and histologically inferior to surface repair in a canine model. J Orthop Res. 2006; 24(5):990–1000. [PubMed: 16514627]

[43]. Thomopoulos S, Zampiakis E, Das R, Kim HM, Silva MJ, Havlioglu N, et al. Use of a magnesium-based bone adhesive for flexor tendon-to-bone healing. J Hand Surg Am. 2009; 34(6):1066–73. [PubMed: 19643291]

[44]. Silva MJ, Boyer MI, Ditsios K, Burns ME, Harwood FL, Amiel D, et al. The insertion site of the canine flexor digitorum profundus tendon heals slowly following injury and structure repair. J Orthop Res. 2002; 20:447–453. [PubMed: 12038617]

[45]. Lieber RL, Amiel D, Kaufman KR, Whitney J, Gelberman RH. Relationship Between Joint Motion and Flexor Tendon Force in the Canine Forelimb. J Hand Surg Am. 1996; 21(6):957–962. [PubMed: 8969415]

[46]. Lieber RL, Silva MJ, Amiel D, Gelberman RH. Wrist and digital joint motion produce unique flexor tendon force and excursion in the canine forelimb. J Biomech. 1999; 32(2):175–181. [PubMed: 10052923]

[47]. Maganaris CN, Paul JP. In vivo human tendon mechanical properties. J Physiol. 1999; 521(1999):307–13. Pt 1. [PubMed: 10562354]

[48]. Raghavan SS, Woon CYL, Kraus A, Megerle K, Choi MSS, Pridgen BC, et al. Human Flexor Tendon Tissue Engineering: Decellularisation of Human Flexor Tendons Reduces Immunogenicity in vivo. Tissue Eng Part A. 2012; 18:796–805. [PubMed: 22011137]

[49]. Kondratko-Mittnacht J, Duenwald-Kuehl S, Lakes R, Vanderby R. Shear Load Transfer in High and Low Stress Tendons. J Mech Behav Biomed Mater. 2015; 45:109–120. [PubMed: 25700261]

[50]. Casey, D.; Lewis, O. Handbook of biomaterials evaluation: scientific, technical and clinical testing of implant materials. Macmillan Publishers Limited; New York, NY: 1986. Absorbable and nonabsorbable sutures; p. 86-94.chap. 7

[51]. Chu, CC.; Von Fraunhofer, JA.; Greisler, HP. Wound closure biomaterials and devices. CRC Press; 1996.

[52]. S. Jackson Inc. Supramid product information sheet. 2015. URL: http://www.supramid.com/content/SUPRAMIDEXTRAIIProductInformation.pdf

[53]. Dillard, DA. Fundamentals of stress transfer in bonded systems. In: Pocius, AV., editor. Adhesion science and engineering / series editor. 1. Elsevier; Amsterdam, The Netherlands: 2002.

[54]. Ashby MF. Overview No. 80: On the engineering properties of materials. Acta Metallurgica. 1989; 37(5):1273–1293.

[55]. Ashby MF, Gibson LJ, Wegst U, Olive R. The Mechanical Properties of Natural Materials. I. Material Property Charts. Proc R Soc A. 1995; 450(1938):123–140.

[56]. Wegst UGK, Ashby MF. The mechanical efficiency of natural materials. Philos Mag. 2004; 84(21):2167–2186.

[57]. Pring DJ, Amis AA, Coombs RR. The mechanical properties of human flexor tendons in relation to artificial tendons. J Hand Surg Eur. 1985; 10:331–336.

[58]. Bouten PJ, Zonjee M, Bender J, Yauw ST, van Goor H, van Hest JC, et al. The chemistry of tissue adhesive materials. Prog Polym Sci. 2014; 39:1375–1405.

[59]. Trail IA, Powell ES, Noble J, Crank S. The role of an adhesive (Histoacryl) in tendon repair. J Hand Surg-Brit Eur. 1992; 17(5):544–9.

[60]. Nassif AC. An Adhesive for Repair of Tissues: Experiments with Canine Tendon, Bone, Lung, Blood Vessels and Skin, Using a Methyl 2-Cyanoacrylate Adhesive. J Surg Res. 1965; 5(3):108–115. [PubMed: 14273765]

[61]. Inoue T, Taguchi T, Imade S, Kumahashi N, Uchio Y. Effectiveness and biocompatibility of a novel biological adhesive application for repair of meniscal tear on the avascular zone. Sci Tech Adv Mater. 2012; 13(6):064219.

[62]. Thomopoulos S, Williams GR, Gimbel JA, Favata M, Soslowsky LJ. Variation of biomechanical, structural, and compositional properties along the tendon to bone insertion site. J Orthop Res. 2003; 21(3):413–9. [PubMed: 12706013]

[63]. Genin GM, Kent A, Birman V, Wopenka B, Pasteris JD, Marquez PJ, et al. Functional grading of mineral and collagen in the attachment of tendon to bone. Biophys J. 2009; 97(4):976–85. [PubMed: 19686644]

[64]. Liu Y, Thomopoulos S, Chen C, Birman V, Buehler MJ, Genin GM. Modelling the mechanics of partially mineralized collagen fibrils, fibres and tissue. J R Soc Interface. 2014; 11(92): 20130835. [PubMed: 24352669]

[65]. Liu Y, Thomopoulos S, Birman V. Bi-material attachment through a compliant interfacial system at the tendon-to-bone insertion site. Mech Mater. 2012; 44:83–92.

[66]. Ming-Yuan H, Hutchinson JW. Crack deflection at an interface between dissimilar elastic materials. Int J Solids Struct. 1989; 25(9):1053–1067.

[67]. Genin GM, Hutchinson JW. Composite laminates in plane stress: constitutive modeling and stress redistribution due to matrix cracking. J Am Ceram Soc. 1997; 80(5):1245–1255.

[68]. McNulty JC, Zok FW, Genin GM, Evans AG. Notch-sensitivity of fiber-reinforced ceramic-matrix composites: Effects of inelastic straining and volume-dependent strength. J Am Ceram Soc. 1999; 82(5):1217–1228.

[69]. Kelly A, Tyson WR. Tensile properties of fibre-reinforced metals: copper/tungsten and copper/molybdenum. J Mech Phys Solids. 1965; 13(6):329–350.

[70]. Gibson, RF. Principles of composite material mechanics. 3. CRC Press; 2011.

[71]. Lekhnitskiĭ, S. Theory of elasticity of an anisotropic elastic body. Holden-Day; San Francisco, CA: 1963.

[72]. Birman V. Mechanics and energy absorption of a functionally graded cylinder subjected to axial loading. Int J Eng Sci. 2014; 78:18–26.

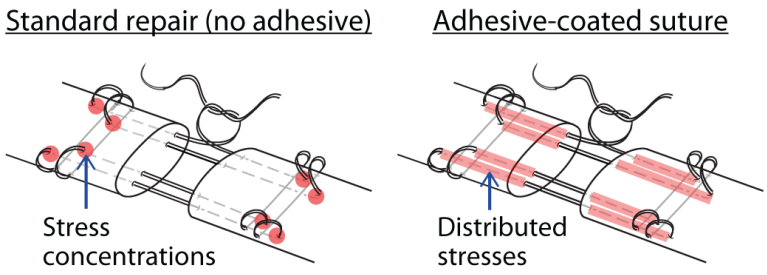

Figure 1.

An 8-stranded Winters-Gelberman suture repair technique is shown for human flexor digitorum profundus tendon repair [11]. Red shading indicates location of load transfer. Current suturing techniques generate stress concentrations at anchor points where the suture bends within tissue. Adhesive-coated sutures could distribute that load transfer along the entire length of the suture, reducing peak stresses and improving overall repair construct mechanics.

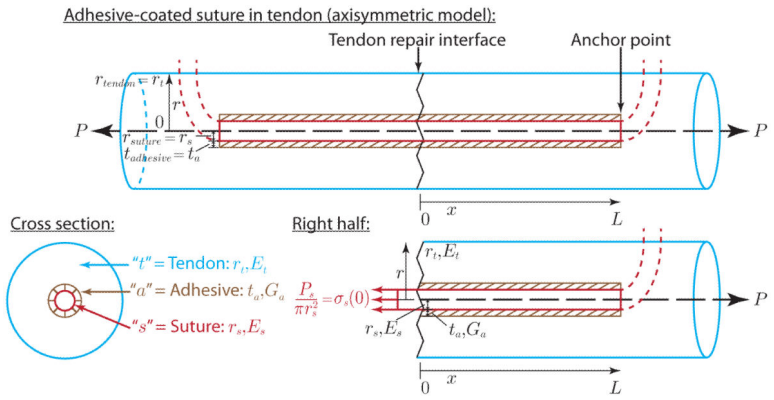

Figure 2.

Diagram of adhesive-coated suture assembly within a cylindrical tissue, such as tendon, used to conduct shear lag analysis. P_s is the tensile load carried by the suture at the interface between repaired tissues (i.e., at $x = 0$). P_k is the load at an anchor point or knot, where the suture bends within the tissue ($x = L$). This load, when too high, leads to the assembly cutting through surrounding tissue and to rupture of the repair.

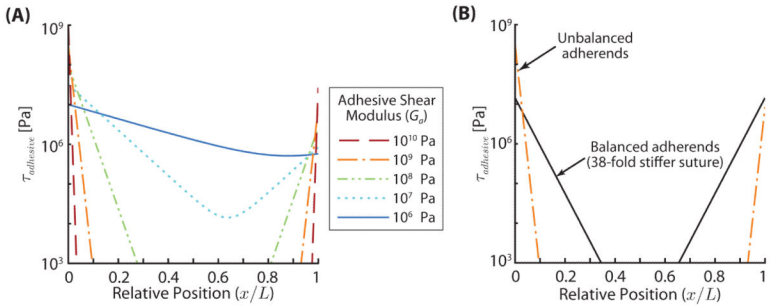

Figure 3.

Shear stress vs. position along the length of a suture is shown. (A) The peak shear stress decreases as the adhesive shear modulus decreases because compliant adhesives distribute loads over a longer distance than stiffer adhesives. (B) A typical repair with Supramid or other sutures is unbalanced in the shear lag sense (i.e., $\rho_t^{*2} > E_s^*$, orange line, G_a = 1 GPa), resulting in higher peak stresses. If a 38x stiffer suture were available to balance the adherends (black line, still using G_a = 1 GPa), the peak stress would drop by a factor of 8.5. In these calculations P_k = 0 N, so that all of the load carried by the suture was transferred to the surrounding tissue via the adhesive.

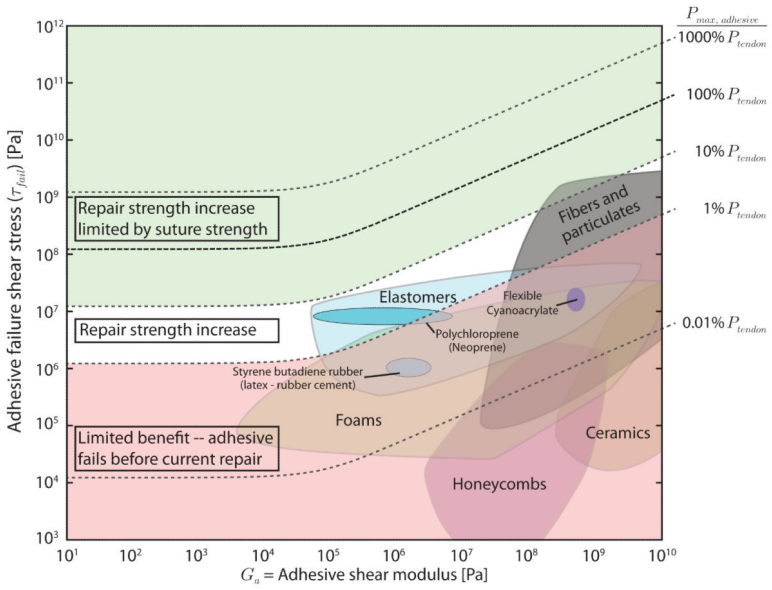

Figure 4.

Contour map of maximum load transferred across the repair by an adhesive-coated suture strand, calculated from a wide array of theoretical adhesive shear moduli and adhesive failure shear stresses (i.e., strengths) given properties described in the methods, and overlaid with real material properties for several material types [25, 26, 27, 28, 54, 55, 56]. Maximum load transfer isoclines were normalized by the strength of healthy human flexor tendons ($P_{tendon} \approx 1000$ N) [57]. Maximum load transfer occurred with an infinitely compliant and infinitely strong adhesive, toward the upper left corner of this contour plot. Current flexor tendon repairs carry approximately 10 N per suture strand, so relevant adhesive coatings would have failure loads above this level. Adhesive mechanical properties that are not expected to improve load transfer are shaded red (lower portion). Note that the suture strand itself breaks above approximately 15.5 N for Supramid 4-0 or 23.5 N for Supramid 3-0 suture [38], so adhesive failure loads above this level would not further improve load transfer (shaded green, upper portion). Also note that shear modulus and failure shear stress are related for a given real material, so not all theoretical combinations are realistic.

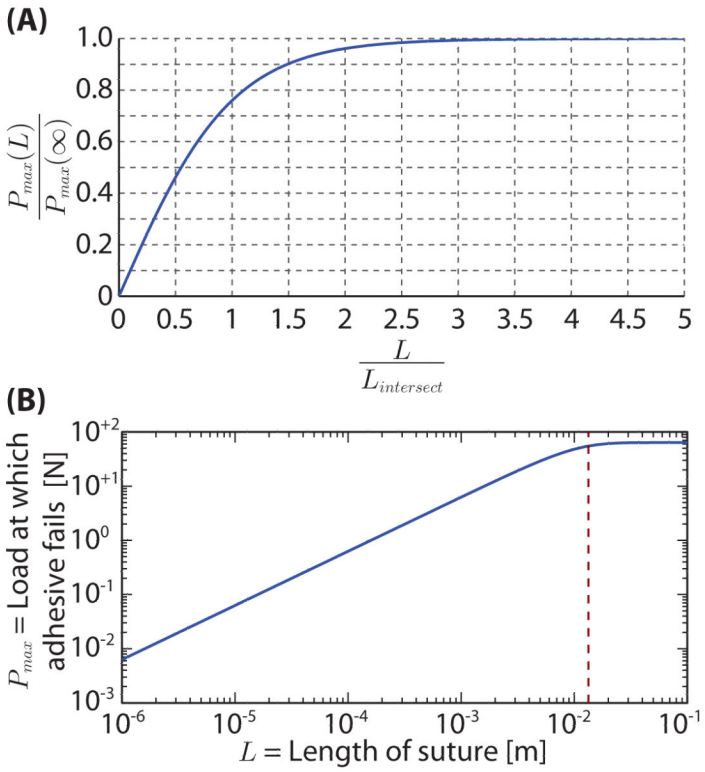

Figure 5.

Increasing suture length increases maximum load carried by assembly, i.e., load causing adhesive to fail, only until a point. Above a transitional suture length, load capacity is governed by an asymptote independent of suture length. (A) Maximum load carried by an assembly, P_{max}, as a function of suture length, L, with respect to the length $L_{intersect}$. Maximum load is normalized by the maximum load transferred by an infinitely long suture, $P_{max}(\infty)$. At $L = L_{intersect}$, the maximum load is 76.0% of the asymptotic maximum load for an infinitely long suture. Note that this is an invariant curve that is true for any combination of t_a, G_a, E_s, r_s, E_t, and r_t that yields a particular value of $L_{intersect}$. (B) Maximum load carried by an assembly as a function of suture length for particular suture, tendon, and adhesive material and geometric properties relevant to flexor tendon repair. Here the adhesive failure shear stress τ_{fail} = 10 MPa, adhesive shear modulus G_a = 100 kPa, adhesive thickness t_a = 0.1 mm, and P_k = 0 N. Current suture length used in flexor tendon repair is 13 mm into each tendon end, as denoted by the dashed line.

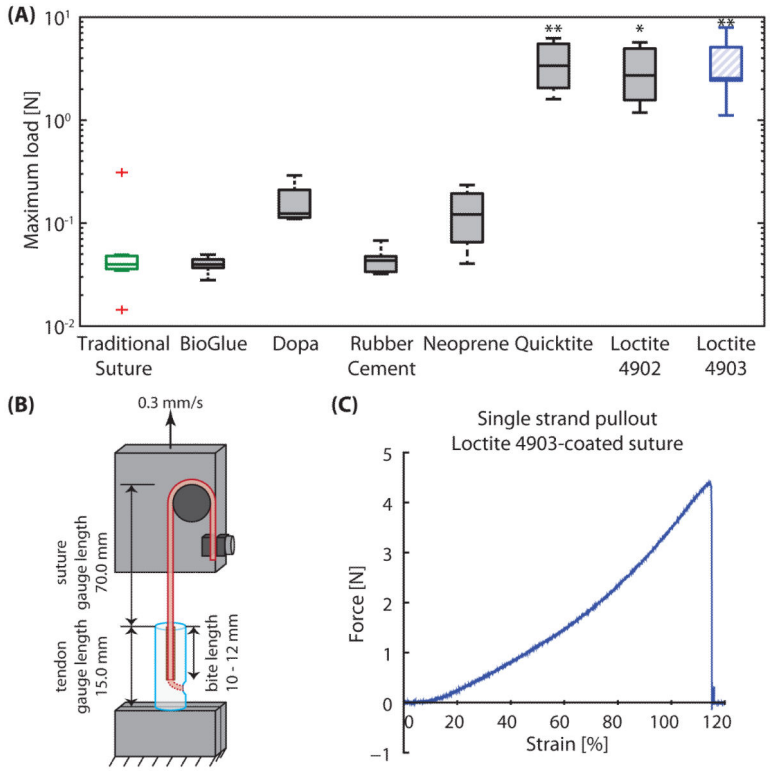

Figure 6.

(A) Maximum loads resisted by single 4-0 Supramid suture strands coated with nothing (traditional suture), CryoLife BioGlue, Dopamine, Elmer's rubber cement, 3M rubber and gasket adhesive 1300 (neoprene), Loctite Quicktite (cyanoacrylate), Loctite 4902 or Loctite 4903 (flexible cyanoacrylates) in cadaveric canine flexor digitorum profundus tendon. The middle line within the box plots represents the median, the outer edges denote the 25 percentile and 75 percentile samples, and the whiskers extend to the extreme data points. Outliers are denoted by (+). Asterisks denote statistically significant differences compared to traditional suture (* $p < 0.05$, ** $p < 0.01$). (B) Schematic of testing setup for single strand adhesive-coated suture pullout from tendon. (C) Representative force-elongation curve for Loctite 4903-coated suture pullout.

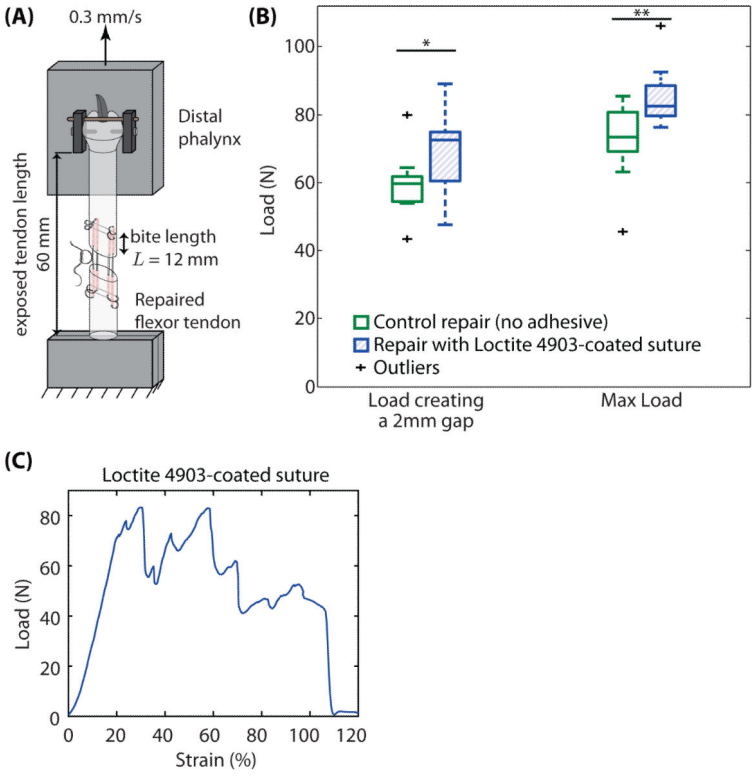

Figure 7.

Tendon repair load tolerance with and without adhesive. (A) Schematic of testing setup for clinically relevant repairs with adhesive-coated suture. (B) The plot shows load creating a 2 mm gap and maximum load for a cadaveric canine flexor digitorum profundus tendon repair using standard clinical surgical technique (8 stranded repair with 4-0 Supramid suture, green) compared with the same repair style where suture was coated with Loctite 4903 (cyanoacrylate adhesive, blue with hash marks). The middle line within the box plots represents the median, the outer edges denote the 25 percentile and 75 percentile samples, and the whiskers extend to the extreme data points. Outliers are denoted by (+). Overbars and asterisks denote statistically significant differences (* $p < 0.05$, ** $p < 0.01$). (C) Representative force-strain curve for 8-stranded repair with Loctite 4903-coated suture.

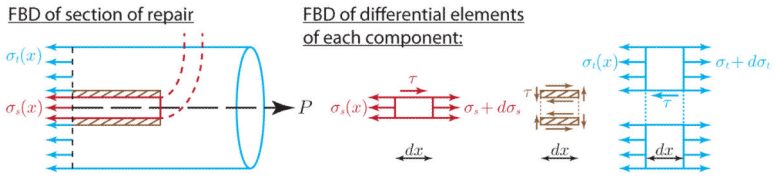

Figure A.8.

Free body diagram showing an axisymmetric model of adhesive-coated suture within a cylindrical tendon tissue. Simultaneously analyzing a section of the repair (left) and each component independently (i.e., suture, adhesive, and tendon; right) allows derivation of a shear lag model to estimate shear stress within the adhesive. Note that this model reduces to a one-dimensional set of equations along the x-axis.

Table 1

Abbreviations and variables used throughout the manuscript.

PBS	Phosphate buffered saline	x	position along suture
$\tau(x)$	shear stress in the adhesive layer	τ_{ave}	average shear stress
τ_{fail}	failure shear stress of adhesive-coated suture	$\bar{\sigma}_s(x)$	normal stress in suture normalized by normal stress at $x = 0$
E_s	suture elastic modulus	E_s^*	suture elastic modulus normalized by tendon elastic modulus
E_t	tendon elastic modulus	G_a	adhesive shear modulus
G_a^*	adhesive shear modulus normalized by tendon elastic modulus		
L	suture purchase length	$L_{intersect}$	suture length where asymptotic limits for load transfer intersect
P_s	normal force in suture at the interface, $x = 0$	P_k	resultant normal force in suture at the anchor point
r_s	suture radius	r_t^*	tendon radius normalized by suture radius
r_t	tendon radius	ρ_t^*	effective radius of tendon, normalized by suture radius
t_a	adhesive thickness	t_a^*	adhesive thickness normalized by suture radius
β_s	characteristic (inverse) length scale related to geometry and material properties	χ	variable related to geometry and material properties

Table 2

Repair resilience, stiffness, and strain at 20 N load are shown for a cadaveric canine flexor digitorum profundus tendon repair using standard clinical surgical technique (8 stranded repair with 4-0 Supramid suture) compared with the same repair style where suture was coated with Loctite 4903 (cyanoacrylate adhesive). Modified resilience shown here is calculated from the force-strain curve.

	Resilience	Stiffness	Strain at 20 N
Repair with Loctite 4903-coated suture	9.12 ± 2.46 N	27.2 ± 4.4 N/mm	8.00 ± 1.36%
Control repair (no adhesive)	7.39 ± 2.22 N	24.0 ± 7.0 N/mm	8.81 ± 2.91%
***p*-value**	0.108	0.251	0.438